



**HAL**  
open science

## Oxygen traces impact on biological methanation from hydrogen and CO<sub>2</sub>

Pierre Buffière, Diana Amaya Ramirez, Ruben Teixeira Franco, Julie Figueras, Stéphane Hattou, Hassen Benbelkacem

### ► To cite this version:

Pierre Buffière, Diana Amaya Ramirez, Ruben Teixeira Franco, Julie Figueras, Stéphane Hattou, et al.. Oxygen traces impact on biological methanation from hydrogen and CO<sub>2</sub>. *Bioresource Technology*, 2025, 419, pp.132080. <10.1016/j.biortech.2025.132080>. <hal-05245003>

**HAL Id: hal-05245003**

**<https://hal.science/hal-05245003v1>**

Submitted on 8 Sep 2025

HAL is a multi-disciplinary open access archive for the deposit and dissemination of scientific research documents, whether they are published or not. The documents may come from teaching and research institutions in France or abroad, or from public or private research centers.

L'archive ouverte pluridisciplinaire HAL, est destinée au dépôt et à la diffusion de documents scientifiques de niveau recherche, publiés ou non, émanant des établissements d'enseignement et de recherche français ou étrangers, des laboratoires publics ou privés.



HAL Authorization

# Oxygen traces impact on biological methanation from hydrogen and CO<sub>2</sub>

Pierre Buffière<sup>1</sup>, Diana Amaya Ramirez<sup>2</sup>, Ruben Teixeira Franco<sup>2</sup>, Julie Figueras<sup>1</sup>, Stéphane Hattou<sup>2</sup>,  
Hassen Benbelkacem<sup>1</sup>

<sup>1</sup>INSA Lyon, DEEP, UR7429, 69621 Villeurbanne Cedex, France

<sup>2</sup>Arkolia Energies, 16 Rue des Vergers, 34130 Mudaison, France

Corresponding author: Pierre BUFFIERE, Professor, INSA Lyon, DEEP, UR7429, 69621 Villeurbanne  
Cedex, France. pierre.buffiere@insa-lyon.fr; +33 (0)4 72 43 84 78

## Abstract

Biomethane production from biological methanation of CO<sub>2</sub> is promising both for biogas upgrading and surplus renewable energy storage. One of the questions for process upscaling is the impact of oxygen (in the biogas or in the purified CO<sub>2</sub>-rich off-gas) on the biological process. An adapted anaerobic thermophilic consortium was submitted to increasing amounts of oxygen in batch and continuous tests at partial pressures ranging from 0 to 50 mbar. Oxygen was quickly consumed and hydrogen uptake remained similar. In the same time, methane production dropped (-4% in continuous tests). Part of the oxygen introduced was reduced biologically by hydrogen. The amount of hydrogen diverted to oxygen reduction (up to 15% at 50 mbar O<sub>2</sub>) was proportional to the oxygen partial pressure. These results suggest that biological methanation systems tolerate the presence of oxygen. However, additional hydrogen should be added to maintain the conversion of CO<sub>2</sub> into methane.

*Keywords: biomethane, biological methanation, oxygen, hydrogen conversion*

---

24 **1. Introduction**

25 Biomethane plays a strategic role in European energy policy, particularly in the context of the  
26 transition towards more sustainable energy sources and the reduction of reliance on fossil fuels. It is  
27 commonly produced through the anaerobic digestion of organic waste (agricultural, industrial,  
28 household). It is particularly important in achieving the European Union's climate goals, including  
29 reaching carbon neutrality by 2050 as claimed by the European Green Deal and related EU directive  
30 2023/2413. Biomethane can be injected directly into existing natural gas networks, allowing for the  
31 gradual replacement of fossil gas with a renewable alternative, without requiring any modifications  
32 of the infrastructure. Biomethane plays a key role in achieving these targets, particularly through the  
33 REPowerEU plan, with an objective of 35 bcm (billions of cubic meter) by 2030 (European  
34 Commission, 2022).

35 The biogas produced through anaerobic digestion contains methane ( $\text{CH}_4$ ), carbon dioxide ( $\text{CO}_2$ ) and  
36 other trace gases like hydrogen sulfide ( $\text{H}_2\text{S}$ ). Conventional processes for biogas upgrading are  
37 generally based on a process unit aimed at separating methane from the other gases in order to  
38 meet the requirements for biomethane injection in the gas grid (Angelidaki et al., 2018). In this  
39 context, the methanation reaction (ie, the conversion of carbon dioxide  $\text{CO}_2$  and hydrogen  $\text{H}_2$  into  
40 methane  $\text{CH}_4$ ) is an emerging pathway for upgrading biogas since it can convert the  $\text{CO}_2$  present in  
41 the biogas (or  $\text{CO}_2$ -rich off-gas from the separation unit) into  $\text{CH}_4$  instead of losing it. The  
42 methanation process can be advantageously combined with  $\text{H}_2$  production from surplus renewable  
43 electricity in a Power to Gas mode (Götz et al., 2016; Thema et al., 2019).

44 Recently, the biological methanation process has been extensively investigated in the context of  $\text{CO}_2$   
45 or biogas upgrading (Chatzis et al., 2024; Lecker et al., 2017; Rafrafi et al., 2021). One of the main  
46 advantage over the catalytic route is that the biological process can be operated in milder conditions  
47 of temperature, and exhibits a higher tolerance to biogas impurities (Figueras et al., 2023). The  
48 biological methanation process has proven its efficiency in terms of performance and flexibility at the

49 demonstration scale (Jønson et al., 2022, Feickert Fenske et al., 2023). It is also a valuable technique  
50 in terms of environmental impact and economy, even if the scalability of the process is however  
51 limited by the cost of energy for hydrogen production (Vinardell et al., 2024).

52 Nevertheless, many biological methanation projects are facing an issue that has not been addressed  
53 so far, which is the question of the presence of oxygen traces in the different gas streams. In biogas  
54 plants for instance, many operators are using micro-aeration to mitigate the production of hydrogen  
55 sulfide (Chen et al., 2020). Alternatively, when methane is separated from the other gases upstream,  
56 the CO<sub>2</sub>-rich off-gas also contains oxygen (Rodin et al., 2020). The data from an industrial biological  
57 methanation project developed by Arkolia Energy show that oxygen is present with both gas type  
58 compositions (0.2% in CO<sub>2</sub>-rich off-gas after methane separation and 0.1% in raw biogas, [see](#)  
59 [supplementary material](#)). This means that in both cases (direct biomethanation of raw biogas or  
60 biomethanation of CO<sub>2</sub>-rich off-gas), oxygen is present in the gas stream. Additionally, the hydrogen  
61 produced by the electrolysis unit may also contain some oxygen traces due to oxygen transfer in the  
62 membrane during electrolysis, and a higher purity of the hydrogen stream means a higher cost for H<sub>2</sub>  
63 production (Martin et al., 2021; Trinke et al., 2017). Even if the gas compositions are relatively poor  
64 in terms of oxygen content, it is important to note that the operating pressure of biological  
65 methanation units are elevated (frequently over 10 bars). For instance, if the O<sub>2</sub> gas composition is  
66 0.1%, this means that the O<sub>2</sub> partial pressure in the biomethanation unit operating at 10 bars would  
67 be 10 mbar.

68 Biological methanation is performed by anaerobic methanogenic archaea in pure culture or in  
69 consortia. In the latter case, the inoculum source generally comes from an anaerobic digester.  
70 Methanogenic organisms are traditionally considered strict anaerobes. However, anaerobic consortia  
71 are known to tolerate the presence of oxygen to some extent (Lu and Imlay, 2021). For example, in  
72 thermophilic anaerobic reactors, low oxygen levels have minimal impact, but at higher  
73 concentrations (4.3–8.8 mg/L), methane production decreases by 40%, and the methanogenic

74 community's development is slowed, though this inhibition is reversible (Pedizzi et al., 2016). Indeed,  
75 in anaerobic digestion consortia, the presence of facultative aerobic organisms helps to eliminate  
76 oxygen to secure strict anaerobic conditions for methane production (Magdalena et al., 2022). In  
77 addition, some acetoclastic methanogens have also shown some skills in adapting to oxidative  
78 stresses (Horne and Lessner, 2013). In pure cultures, exposing hydrogenotrophic archaea to oxygen  
79 may lead to lower viability of the cells, even if some of them able to grow in the presence of oxygen,  
80 especially *M. thermoautotrophicum*, which is commonly encountered in biomethanation reactors  
81 (Kiener and Leisinger, 1983). Some of them also have the ability not only to grow, but also to use  
82 oxygen by developing a specific metabolism able to reduce oxygen (Tholen et al., 2007) and, in the  
83 presence of hydrogen, to produce water (Seedorf et al., 2004), in the detriment however to their  
84 methanogenic metabolism.

85 All collected data so far come from pure culture of dedicated archaea, or from anaerobic digestion of  
86 organic biomass. To our knowledge, there have been no investigation on biological methanation  
87 reaction on short-term or long term (continuous) operation. The present study focused on the  
88 implementation of a thermophilic microbial consortium for biological methanation, which was  
89 exposed to increasing amounts of oxygen. The experiments were carried out in batch and continuous  
90 mode and monitored for the conversion balances of the gases introduced ( $O_2$ ,  $CO_2$  and  $H_2$ ) and the  
91 methane produced. The aim was to assess the oxygen tolerance of the biomethanation process up to  
92 a partial pressure of 50 mbar, which is well beyond the upper limit that can be encountered  
93 industrially.

## 94 **2. Materials and Methods**

95 The experimental strategy relies on batch and continuous tests. Batch tests (see section 2.1) enables  
96 to understand the dynamics of the evolution of the different gases. The tests were performed with 4  
97 levels of oxygen partial pressure ranging from 0 (control) to 50 mbar (Table 1). The continuous tests  
98 were performed on a 10 L reactor. Three different oxygen levels were tested (2, 5 and 10 mbar) over  
99 operating periods ranging from 6 to 18 days (see section 2.2). The continuous reactor medium was  
100 used as the inoculum source for the batch tests.

### 101 **2.1 Batch tests setup**

102 The methodology used for the batch test was adapted from activity measurements with gaseous  
103 substrates (Figueras et al., 2023; Laguillaumie et al., 2023). The tests were carried out in triplicate  
104 with 500 mL bottles (Schott) filled with 180 g of inoculum. The bottles were first bubbled with  
105 nitrogen for 10 minutes and with a standard gas bottle (Linde, France) containing N<sub>2</sub>: 50%, H<sub>2</sub>: 40%,  
106 CO<sub>2</sub>: 10%, for 8 minutes. The presence of nitrogen was necessary to prevent the pressure to drop  
107 below the ambient pressure, as the gas mole number decreases during the methanation reaction.  
108 The initial pressure in the bottles was set at 1900 mbar. Butyl rubber septa and screw tops were used  
109 to seal the bottles. Then, a known volume of air was injected into the bottles with a needle to adjust  
110 the desired initial oxygen partial pressure. All bottles were placed at 55°C in an orbital shaker  
111 incubator (110 rpm). The gas headspace pressure and composition were monitored for 3 days. The  
112 initial partial pressure in the bottles headspace for each condition is shown in Table 1. For the  
113 calculations, the total pressure measured was corrected for the water partial pressure.

114 The inoculum used for came from the continuous 10L reactor (see next section). The initial TS  
115 content was 3.8 g/L and VS content 3.1 g/L, initial pH was 7.12 and N-NH<sub>4</sub><sup>+</sup> initial concentration was  
116 0.33 g<sub>N</sub>/L. The soluble phase of the inoculum (after filtration at 0.45μ) provided all the necessary  
117 elements (sulfur and trace metals) as revealed by ICP-OES measurement (see supplementary  
118 material).

## 119 2.2 Continuous Reactor setup and operating conditions

120 The continuous reactor is a stirred column as schematized in Figure 1. This technology was preferred  
121 to the trickled bed reactor (TBR) system by Arkolia Energies based on its economical balance, even if  
122 TBR have been intensively investigated as efficient systems for this application, notably for mass  
123 transfer performances (Jensen et al., 2021b; Orgill et al., 2013; Strübing et al., 2017). In addition,  
124 using free-suspended cell systems in both batch and continuous experiments was found more  
125 appropriate for the present study. Indeed, in biofilm systems like TBR, the impact of oxygen may not  
126 be as important due to the protection effect and diffusion limitations in the biofilm (Dupnock and  
127 Deshusses, 2019).

128 The reactor consists of a glass jacketed column with 600 mm height and 150 mm inner diameter  
129 (total volume 10.6 L). It was operated at atmospheric pressure and the liquid height was regulated at  
130 500 mm by hydrostatic pressure using a U-shaped plastic tube filled with liquid and open to external  
131 atmosphere. This allowed the working volume to be fixed at 8.8 L and at the same time to recover the  
132 excess liquid obtained from biological water production and nutrient solution addition. The reactor  
133 was equipped with four standard baffles (12 mm diameter and 4 mm wall clearance) and two 800  
134 mm diameter radial impellers (Ekato, Germany) mounted on a vertical stirrer shaft (500 mm working  
135 length and 120 mm diameter). Stirring was controlled by an electric engine (Heidolph Instruments,  
136 Germany) connected to a magnetic coupling (Büchi AG, Switzerland). Temperature in the reactor was  
137 controlled at  $55.0 \pm 0.3$  °C with a thermostatic water bath circulator (Julabo, Germany). A peristaltic  
138 pump (MasterFlex, USA) was used to control the flowrate of the nutrient solution added to the  
139 reactor, macro and micronutrient solution (S1) and sulfur solution (S2) are added separately (Figure  
140 1), 150 mL per day of each solution were injected in the reactor (see supplementary materials for the  
141 composition of S1 and S2).

142 Process gases were injected at the bottom of the reactor through a sintered gas diffuser. H<sub>2</sub> (>  
143 99.9995%) was produced in-situ through a H<sub>2</sub> generator (F.DGSi, France) and CO<sub>2</sub> (> 99.9%) was

144 provided from gas bottle (Air Liquide, France). For H<sub>2</sub>, CO<sub>2</sub> and O<sub>2</sub> inlet gas flow were regulated by an  
145 independent mass flow controller (Brooks Instrument, USA). Airflow was injected with an air  
146 compressor MXF08-10T/20L (Mauguière, Italy) and pure nitrogen was injected with an on-site  
147 nitrogen generator NG4-1DC (Noblegen, United Kingdom). Outlet gas (top of the column) passed  
148 through a foam trap bottle, and it was dried in a cold-water bath, model F12, at 10 ± 1 °C (Julabo,  
149 Germany). The flow rate of dried outlet gas was measured by a drum-type gas meter (Ritter,  
150 Germany).

151 The reactor was initially inoculated with a mesophilic digested sludge provided by a nearby  
152 wastewater treatment plant (La Feysine WWTP, Villeurbanne, France). Prior to this study, it had been  
153 operated for 690 days with an input gas (80% H<sub>2</sub> / 20% CO<sub>2</sub>) ranging from 5 to 15 NL/h in thermophilic  
154 conditions. The operational conditions are presented in Table 2. They were selected according to the  
155 nominal operating conditions (10 NL/h, ie., 8 NL/h of H<sub>2,in</sub> and 2 NL/h of CO<sub>2,in</sub>). The first period  
156 (control period) lasted 28 days in stable conditions (condition 1). Then, for 14 days air was injected  
157 with an oxygen partial pressure of 10 mbar (condition 2). Then, oxygen partial pressure was switched  
158 to condition 3 (5 mbar) and 4 (2 mbar) successively. Two additional conditions with nitrogen alone  
159 were used (conditions 5 and 6). The total gas flow rate was thus comprised 10 and 10.5 L/h, which  
160 correspond to a gas retention time between 3000 and 3170 seconds on empty reactor volume (450  
161 to 475 seconds gas residence time with an average gas holdup of 1.5%). The idea behind conditions 5  
162 and 6 tests was to operate the reactor with a N<sub>2</sub> partial pressure similar to that used with oxygen in  
163 order to check the influence of dilution effects on the performances with an inert gas. The duration of  
164 each operation can be different based on several practical issues, but the criteria used was to get  
165 several successive stable days of operation with all measurements available. The data used for mass  
166 balance calculations (detailed in section 2.4) were taken during stable operation periods: constant  
167 outlet gas flow rate and composition (usually 5 days, except for condition 5 where only 2 days data  
168 have been used).

169 **2.3 Analytical methods**

170 For the batch tests, the gas composition was analyzed by gas chromatography (Global Analyser  
171 Solutions G.A.S, Netherlands) with thermal conductivity detector (GC-TCD). Molsieve 5A 0.32 mm ID  
172 (10 m length) and Rt-U-Bond (10 m length; 0.32 mm ID) columns were used as stationary phases for  
173 GC-TCD, with Argon as carrier gas, for both columns. Headspace pressure was measured with a  
174 precision electronic manometer (Digitron 2025P7).

175 For continuous tests, the composition of outlet gas was measured every 15 minutes by a micro gas  
176 chromatography (Inficon, Switzerland) with thermal conductivity detector (GC-TCD). Rt-Molsieve 5A  
177 0.25 (12 m length) and RT-Q-Bond (12 m length; 0.25 mm ID) columns were used as stationary phases  
178 for GC-TCD, with Argon and Helium as carrier gases, respectively. Temperature and pH of liquid inside  
179 the reactor were measured on-line with a thermocouple type J (TC direct, France) and an easySense  
180 31 pH probe (Mettler Toledo, USA), respectively. Redox potential was measured with a redox probe  
181 HI3210B/5 (Hanna Instruments, USA). The liquid output from biological water production and  
182 nutrient management was collected in a 2 L glass bottle and weighed on average twice a week.

183 **2.4. Calculations and hypothesis**

184 All calculations are performed on a molar basis. In the batch tests, the number of moles for each gas  
185 component is calculated from the ideal gas state equation:

186 
$$n_i = \frac{p_i V_h}{RT} \quad (1)$$

187 Where  $p_i$  is the gas partial pressure in Pa (calculated from total pressure and gas composition  
188 measurement),  $V_h$  is the headspace volume in  $\text{m}^3$  and  $T$  the temperature (K). For the continuous  
189 tests, a similar approach is used: when the reactor operation is stable, the cumulated inlet and outlet  
190 mole number of each gas was calculated through the cumulated volume, temperature, operating  
191 pressure and gas composition. Since the water composition of the gas is not measured, the total  
192 pressure used for the calculations is the dry pressure (corrected for water pressure at the operating  
193 temperature).

194 The global conversion efficiencies  $X_{i,conv}$  of carbon dioxide and hydrogen are then calculated as follow:

195 
$$X_{i,conv} = \frac{n_{i,in} - n_{i,out}}{n_{i,in}} \quad (2)$$

196 In this equation,  $n_{i,in}$  is the initial (in batch mode) or inlet (in continuous mode) mole number of each  
197 gas, and  $n_{i,out}$  is the final (in batch mode) or outlet (in continuous mode) mole number.

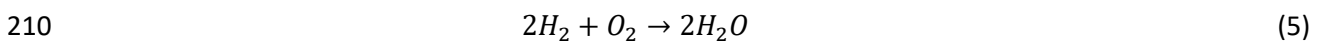
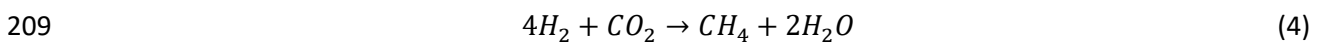
198 Similarly, the product (methane) yield (in  $\text{mol}_{\text{CH}_4} \cdot \text{mol}_{\text{H}_2}^{-1}$ ) was calculated as the ratio between the  
199 amount of methane produced divided by the amount of hydrogen consumed:

200 
$$Y_{\text{CH}_4} = \frac{n_{\text{CH}_4,out}}{n_{\text{H}_2,in} - n_{\text{H}_2,out}} \quad (3)$$

201 In this expression,  $n_{\text{CH}_4,out}$  is the molar amount of methane produced and  $n_{\text{H}_2,in} - n_{\text{H}_2,out}$  represent  
202 the amount of hydrogen converted.

203 Based on the results obtained, it appeared that the uptake of hydrogen could be associated not only  
204 to the methanogenic reaction, but also to the oxygen reduction reaction. In order to evaluate how  
205 hydrogen was used, we assumed that the following mechanisms took place:

- 206 - The catabolic reaction of hydrogenotrophic methanogenesis (equation 4);  
207 - The catabolic reaction of oxygen reduction (equation 5);  
208 - Other metabolic reactions (growth, maintenance).



211 The production of methane during the tests enables to calculate the fraction of hydrogen used for  
212 methane production through reaction 1 ( $f_{\text{H}_2,\text{CH}_4}$ ):

213 
$$f_{\text{H}_2,\text{CH}_4} = \frac{4 \times n_{\text{CH}_4,out}}{n_{\text{H}_2,in} - n_{\text{H}_2,out}} \quad (6)$$

214 Similarly, the uptake of oxygen enables to estimate the fraction of hydrogen used for oxygen  
215 reduction through reaction 2 ( $f_{\text{H}_2,\text{O}_2}$ ), where  $n_{\text{O}_2,in} - n_{\text{O}_2,out}$  is the molar amount of oxygen  
216 removed.

217 
$$f_{H_2,O_2} = \frac{2 \times (n_{O_2,in} - n_{O_2,out})}{n_{H_2,in} - n_{H_2,out}} \quad (7)$$

218 The remaining fraction of hydrogen removed  $f_{H_2,other}$  is thus considered as what is used for other  
 219 metabolic routes:

220 
$$f_{H_2,other} = 1 - f_{H_2,CH_4} - f_{H_2,O_2} \quad (8)$$

221 If some of the hydrogen is used for oxygen reduction, then the observed methane yield defined in  
 222 equation 3 should be lower than without oxygen. In order to take this effect into account, a  
 223 correction was used to calculate the actual methane yield of the methanogenic reaction. With the  
 224 assumption that 1 mole of oxygen consumed 2 moles of H<sub>2</sub>, the corresponding amount of hydrogen  
 225 available for methanogenesis is reduced (equation 9).

226 
$$Y_{CH_4,corr} = \frac{n_{CH_4,out}}{(n_{H_2,in} - n_{H_2,out}) - 2 \times (n_{O_2,in} - n_{O_2,out})} \quad (9)$$

227 For batch test, uncertainties were determined from the standard deviation between the replicates.  
 228 For continuous operations, uncertainties were determined from the standard deviation of the  
 229 measured quantities during stable operation periods.

### 230 **3. Results and discussion**

#### 231 **3.1 Batch test**

232 Figure 2 presents the evolution of the headspace composition (amount of oxygen, methane, carbon  
 233 dioxide and hydrogen conversion). Oxygen uptake began in the first 0.25 days of the experiment. The  
 234 reactor's headspace was then fully depleted within 0.25 and 1 day for initial partial pressure of 3.8  
 235 mbar and between 1 and 2 days for initial oxygen partial pressure of 23 and 50 mbar. Methane  
 236 production (Figure 2B) started after 0.25 days (at 0 mbar O<sub>2</sub>), but seemed to be all the more delayed  
 237 when the initial amount of oxygen increased. In the same time, H<sub>2</sub> uptake began earlier as shown in  
 238 Figure 2C. It has to be mentioned that due to GC calibration issues associated to H<sub>2</sub> composition,  
 239 there was an important uncertainty on the calculation of H<sub>2</sub> conversion efficiencies when the H<sub>2</sub>  
 240 content in the headspace was high. It can also be noticed that the CO<sub>2</sub> uptake was in line with the

241 production of methane. The maximal methane production was reached after 2 days for the tests  
242 operated at 0 and 3.8 mbar initial  $P_{O_2}$ , and after 3 days  $P_{O_2}$  of 23 mbar (all the hydrogen being  
243 converted). The methane production was not maximal for the tests done at 50 mbar oxygen (only 90  
244 % of the hydrogen was converted for this test after 3 days). Another interesting feature is the  
245 comparison between the amount of hydrogen consumed and the amount of methane produced. In  
246 spite of the calibration issues it was possible to calculate the methane yield  $Y_{CH_4}$ , since the initial  
247 amount of hydrogen was known and the final amount was accurately measured. The amount of  
248 hydrogen consumed, methane produced and the calculated methane yield are presented in Table 3.  
249 The results show that the methane yield was directly affected by the presence of oxygen. It is  
250 dropping from 0.248 (without oxygen) to 0.209 (at 50 mbar initial  $P_{O_2}$ ). The values are consistent with  
251 the expected yield, since the stoichiometry of the catabolic methanogenesis reaction (equation 4)  
252 predicts a maximal yield of 0.25. This result shows that, in the presence of oxygen, some of the  
253 hydrogen was not used for methanogenesis. The decrease of the methane yield, together with the  
254 fact that oxygen was consumed, leads to the hypothesis that some of the hydrogen could be derived  
255 towards oxygen reduction (equation 5). In order to check this hypothesis, it was possible to  
256 recalculate the methane yield of the methanogenic reaction by correcting the amount of  $H_2$  used for  
257 oxygen reduction, in order to get a corrected methane yield (equation 9). All values of the corrected  
258 metabolic methane yield of the methanogenesis reaction (last column in Table 3) fall in the same  
259 range, independently of the initial  $P_{O_2}$  (between 0.239 and 0.248, with uncertainties ranging from  
260 0.010 to 0.030). This means that in spite of the presence of oxygen, there were no specific  
261 disturbance of the methanogenic metabolism concerning methane production: only the observed  
262 methane yield (column 4 in Table 3) was affected due to use of hydrogen for oxygen reduction. The  
263 corrected methane yield was very similar to the methane yield of 0.24 estimated with pure culture of  
264 *Methanobacterium Thermoautotrophicum* (Schill et al., 1996), and with the value of 0.23 used in the  
265 model developed for thermophilic methanation in mixed culture (Grimalt-Alemany et al., 2020).

266 These results reveal two important features. First, oxygen was consumed quickly by the micro-  
267 organisms of the thermophilic mixed culture used, even after a long time of acclimatization under  
268 anaerobic conditions. Second, methane production was delayed in the presence of oxygen. In  
269 addition, it is highly probable that some of the microorganisms present in the culture were able to  
270 oxidize hydrogen in the presence of oxygen. As mentioned in section 2.2, the inoculum used for the  
271 batch tests came from the continuous reactor that has been operated for 600 days with H<sub>2</sub> and CO<sub>2</sub>  
272 (and no other energy source than hydrogen). It was thus expected that the microbial consortium was  
273 mostly enriched with thermophilic hydrogenotrophic archaea. It has been shown that some  
274 methanogenic species can survive in the presence of oxygen (Kiener and Leisinger, 1983), and others  
275 are even able to oxidize hydrogen (Tholen et al., 2007). In the present case however, it was difficult  
276 to tell if the aerobic oxidation of hydrogen was done by the dominant archaea or by other bacterial  
277 species. Indeed, some hydrolytic bacterial species present in the mixed culture might have the ability  
278 to use hydrogen aerobically. Nevertheless, it was clear that the onset of methane production was  
279 delayed. This shows either that hydrogen would preferentially be used through an aerobic  
280 metabolism, or that oxygen actually inhibits reversibly the methanogenesis reaction. Some authors  
281 have already noted that the rapid growth of aerobic facultative organisms would probably  
282 outcompete the methanogens for hydrogen uptake due to their higher specific activity and growth  
283 yield (Botheju and Bake, 2011; Pedizzi et al., 2016). Understanding the metabolism of the microbial  
284 community would require further investigations and additional metabolic tools. However, the  
285 question of the resilience of the methanogenic activity is addressed in the next section, where  
286 continuous tests results are presented.

287

### 288 **3.2 Continuous test**

289 The results of the continuous tests are summarized in Table 4. Condition 1 corresponds to the  
290 reference (no gas injected other than H<sub>2</sub> and CO<sub>2</sub>). Conditions 2, 3 and 4 correspond to an additional

291 air sparging at oxygen partial pressures of 10, 5 and 2 mbar, respectively (at the working pressure of  
292 1 bar, these values correspond to oxygen compositions of 1%, 0.5% and 0.2%, respectively).  
293 Conditions 5 and 6 are performed with nitrogen alone instead of air, to reproduce the same gas  
294 dilution effect as for conditions 2 and 3.

295 Hydrogen conversion was high in all tests (over 99%). However, H<sub>2</sub> conversion is slightly lower (98.8 ±  
296 0.2%) for condition 2 (P<sub>O<sub>2</sub></sub>= 10 mbar). This slight difference does not necessarily mean that conversion  
297 has decreased due to the presence of oxygen. Indeed, this value is close to that obtained under the  
298 same conditions with nitrogen instead of air (condition 5, conversion 99.0 ± 0.3%) and could  
299 therefore be attributed to the dilution effect that could impact the hydrogen mass transfer efficiency  
300 by reducing its partial pressure (Jensen et al., 2021a).

301 The conversion efficiency of CO<sub>2</sub> and hydrogen, together with the methane composition in the outlet  
302 gas are plotted in Figure 3. The effect of the presence of oxygen on CO<sub>2</sub> conversion is obvious here.  
303 The rate of CO<sub>2</sub> conversion decreased linearly with the partial pressure of oxygen applied (from  
304 98.8% for reference, to 93.7% for condition 2). Even if the pH conditions are not strictly identical (7.6  
305 for reference and 7.3 for condition 2), they alone do not explain the difference observed.

306 Similarly, the methane composition of the outlet gas decreased with increasing oxygen partial  
307 pressure. In Figure 3, this composition was corrected to eliminate the presence of nitrogen (in  
308 variable amounts depending on the conditions). It should be noted that the methanation reaction  
309 (equation 4) is accompanied by a decrease in flow rate (5 moles of gas disappear for a single mole of  
310 gas produced). Consequently, the presence of nitrogen from the air leads to a variable nitrogen  
311 composition at the outlet (2.8, 12.1 and 20.8% for conditions 4, 3 and 2, respectively). This correction  
312 enables the results to be compared with each other, and shows that the reduction in methane  
313 content is noticeable for conditions 3 and 2 (5 and 10 mbar O<sub>2</sub>). It should also be noted that in all  
314 tests, almost all the oxygen was consumed (Table 4). The presence of traces of oxygen (up to 241

315 ppm, condition 2) in the outlet gas is rather a residue due to the amount that has not transferred  
316 into the liquid phase.

317 Another consequence of the presence of oxygen is the slight decrease in methane productivity, from  
318 5.20 NL.L<sup>-1</sup>.d<sup>-1</sup> for the control, to 5.02 for condition 2 (10 mbar O<sub>2</sub>). Finally, it can be noted that, quite  
319 logically, the oxido-reduction potential (ORP) rose in the presence of oxygen, which is a common  
320 feature of micro-aerated anaerobic systems (Magdalena et al., 2022; Yu et al., 2020).

321 The intermediate conclusions that can be drawn from the continuous tests are as follows. First,  
322 almost all the oxygen was consumed. Second, it appeared that almost all hydrogen was consumed,  
323 while CO<sub>2</sub> conversion decreased concomitantly with the increase in oxygen partial pressure. Finally,  
324 methane production decreased slightly. These findings confirm the results obtained in batch  
325 operation. They also suggest that a metabolism other than methane production is associated with  
326 hydrogen consumption.

327

### 328 **3.3 The fate of hydrogen in the presence of oxygen**

329 From both batch and continuous tests results, there was a correlation between the amount of  
330 oxygen added (and consumed) and the amount of methane produced, while the hydrogen uptake did  
331 not vary. It is thus likely that some of the hydrogen was used to reduce oxygen into water (reaction  
332 5). Indeed, hydrogen is the only available energy source since the reactors are only fed with H<sub>2</sub>, CO<sub>2</sub>  
333 and air. In addition, some methanogens are known to be able to reduce oxygen through the  
334 modification of the F420 cofactor (involved in the methane production) into a F420H<sub>2</sub> oxidase  
335 (Seedorf et al., 2004). This protection mechanism seems to be associated with a stop of the  
336 methanogenic activity, even if it is reversible (Tholen et al., 2007). In the present case, mixed culture  
337 were used. It is thus difficult to tell if the thermophilic methanogens actually changed their  
338 metabolism to reduce oxygen, or if other species present in the microbial consortium are responsible  
339 for this O<sub>2</sub> conversion. A thorough study of the microbial population, focusing on potential shifts  
340 within the communities, could provide further insights. However, it was noticed (Figure 2A) that the

341 oxygen uptake started immediately without any observable lag-phase in batch tests. In continuous  
342 test (Table 4), the oxygen level was very low, suggesting also the ability of the consortium to use  
343 oxygen.

344 Based on this hypothesis, hydrogen and oxygen uptake (on the one hand), and methane production  
345 (on the other hand), were used to calculate how hydrogen was used among methane production,  
346 oxygen reduction, or other anabolic activity (equations 6, 7 and 8). The results are presented on  
347 Figure 4 in batch mode (left) and continuous mode (right). The common feature is that the fraction of  
348 hydrogen used for methane production decreased with increasing oxygen partial pressure. At the  
349 same time, the amount of hydrogen used for other anabolic activities remained stable (given  
350 measurement uncertainties). Finally, the proportion of hydrogen used for oxygen reduction also  
351 increased significantly to reach 15% at 50 mbar  $P_{O_2}$  (batch tests). This fraction was plotted against the  
352 applied oxygen partial pressure (Figure 5). Interestingly, it did not depend on the reactor operation  
353 mode (batch or continuous). In addition, the fraction of hydrogen used for oxygen reduction varied  
354 linearly with the oxygen partial pressure. This result strongly supports the hypothesis of  $H_2$  utilization  
355 for oxygen reduction.

356 In the two sets of experiments, the presence of oxygen at low amounts (below 50 mbar of partial  
357 pressure) did not affect the anaerobic metabolism of hydrogenotrophic methanogens in thermophilic  
358 methanation mixed culture. However, based on mass balance calculations, it was demonstrated that  
359 oxygen was consumed. In the same time, there were evidence that some of the hydrogen present in  
360 the system was preferentially used for oxygen reduction. The consequence for practical applications  
361 is that the applied amount of hydrogen should be increased to make sure that all the  $CO_2$  can be  
362 converted into methane. According to the data presented (Figure 5), in a biomethanation reactor  
363 operating at 10 bars with 0.2% oxygen in the inlet gas (20 mbar  $O_2$ ), 6% of the hydrogen would be  
364 derived for oxygen reduction. It means that the  $H_2/CO_2$  ratio should be increased from 4/1  
365 (stoichiometric value) to 4.24/1 in order to reach the methane yield and productivity that would be

366 obtained without oxygen. Even if this increase is limited, the impact of the presence of oxygen traces  
367 has to be accounted for in the design and operation of biological methanation units.

#### 368 **4. Conclusions**

369 The presence of oxygen (at partial pressures below 50 mbar) did not stop biological methanation.  
370 Oxygen was rapidly consumed. The uptake of hydrogen remained unchanged, while methane  
371 production and CO<sub>2</sub> uptake decreased at higher oxygen pressure. Molar balance showed that up to  
372 15% of the hydrogen was used to reduce oxygen. This fraction increased linearly with oxygen partial  
373 pressure. Low amounts of oxygen in biomethanation system are thus tolerable. However, to  
374 counterbalance the amount of hydrogen diverted to reduce oxygen, it is necessary to increase the  
375 H<sub>2</sub>/CO<sub>2</sub> ratio for maintaining a satisfactory methane productivity and CO<sub>2</sub> conversion.

376

377 E-supplementary data for this work can be found in e-version of this paper online.

#### 378 **Acknowledgements**

379 This work was performed within the framework of the EUR H2O'Lyon (ANR-17-EURE-0018) of  
380 Université de Lyon (UdL), within the program "Investissements d'Avenir" operated by the French  
381 National Research Agency (ANR). It is part of the OCCIBIOM project developed by Arkolia Energies  
382 and co-funded by GrDF in the framework of "green future" project – biogenic CO<sub>2</sub> recovery from  
383 methanisation in Occitanie and Nouvelle-Aquitaine. The authors want to thank the DEEP laboratory  
384 technical team for their support during experiments: Hervé Perier-Camby and Richard Poncet for the  
385 reactor setup and; Nathalie Dumont and David Lebouil for carrying out chemical analysis. Also, we  
386 thank the technical Arkolia laboratory team (NRLab) for carrying out batch tests: Sophie Clerc et Laura  
387 Chatain.

388

389

390

391 **Declaration of generative AI and AI-assisted technologies in the writing process**

392 During the preparation of this work the author(s) used DeepL in order to improve the readability and  
393 language of the manuscript. After using this tool/service, the author(s) reviewed and edited the  
394 content as needed and take(s) full responsibility for the content of the published article.

395 **References**

- 396 Angelidaki, I., Treu, L., Tsapekos, P., Luo, G., Campanaro, S., Wenzel, H., Kougias, P.G., 2018. Biogas  
397 upgrading and utilization: Current status and perspectives. *Biotechnol. Adv.* 36, 452–466.  
398 <https://doi.org/10.1016/J.BIOTECHADV.2018.01.011>
- 399 Botheju, D., Bake, R., 2011. Oxygen Effects in Anaerobic Digestion – A Review. *Open Waste Manag. J.*  
400 4, 1–19. <https://doi.org/10.2174/1876400201104010001>
- 401 Chatzis, A., Gkotsis, P., Zouboulis, A., 2024. Biological methanation (BM): A state-of-the-art review on  
402 recent research advancements and practical implementation in full-scale BM units. *Energy*  
403 *Convers. Manag.* 314, 118733. <https://doi.org/10.1016/j.enconman.2024.118733>
- 404 Chen, Q., Wu, W., Qi, D., Ding, Y., Zhao, Z., 2020. Review on microaeration-based anaerobic digestion:  
405 State of the art, challenges, and prospectives. *Sci. Total Environ.* 710, 136388.  
406 <https://doi.org/10.1016/j.scitotenv.2019.136388>
- 407 Dupnock, T.L., Deshusses, M.A., 2019. Detailed investigations of dissolved hydrogen and hydrogen  
408 mass transfer in a biotrickling filter for upgrading biogas. *Bioresour. Technol.* 290, 121780.  
409 <https://doi.org/10.1016/J.BIORTECH.2019.121780>
- 410 European Commission, 2022. REPowerEU Plan, COM(2022) 230 final ([https://eur-lex.europa.eu/legal-](https://eur-lex.europa.eu/legal-content/EN/TXT/HTML/?uri=CELEX:52022DC0230)  
411 [content/EN/TXT/HTML/?uri=CELEX:52022DC0230](https://eur-lex.europa.eu/legal-content/EN/TXT/HTML/?uri=CELEX:52022DC0230)), COM/2022/230 final.
- 412 Feickert Fenske, C., Strübing, D., Koch, K., 2023. Biological methanation in trickle bed reactors - a  
413 critical review. *Bioresour. Technol.* 385, 129383.  
414 <https://doi.org/10.1016/j.biortech.2023.129383>

415 Figueras, J., Benbelkacem, H., Dumas, C., Buffiere, P., 2023. Inhibitions from Syngas Impurities: Impact  
416 of Common Tar Components on a Consortium Adapted for Syngas Biomethanation. *Waste*  
417 *Biomass Valorization*. <https://doi.org/10.1007/s12649-023-02237-x>

418 Götz, M., Lefebvre, J., Mörs, F., McDaniel Koch, A., Graf, F., Bajohr, S., Reimert, R., Kolb, T., 2016.  
419 Renewable Power-to-Gas: A technological and economic review. *Renew. Energy* 85, 1371–  
420 1390. <https://doi.org/10.1016/j.renene.2015.07.066>

421 Grimalt-Aleman, A., Asimakopoulos, K., Skiadas, I.V., Gavala, H.N., 2020. Modeling of Syngas  
422 Biomethanation and Control of Catabolic Routes of Mesophilic and Thermophilic Mixed  
423 Cultures. *Appl. Energy* 262.

424 Horne, A.J., Lessner, D.J., 2013. Assessment of the oxidant tolerance of *Methanosarcina acetivorans*.  
425 *FEMS Microbiol. Lett.* 343, 13–19. <https://doi.org/10.1111/1574-6968.12115>

426 Jensen, M.B., Ottosen, L.D.M., Kofoed, M.V.W., 2021a. H<sub>2</sub> gas-liquid mass transfer: A key element in  
427 biological Power-to-Gas methanation. *Renew. Sustain. Energy Rev.* 147, 111209.  
428 <https://doi.org/10.1016/j.rser.2021.111209>

429 Jensen, M.B., Poulsen, S., Jensen, B., Feilberg, A., Kofoed, M.V.W., 2021b. Selecting carrier material for  
430 efficient biomethanation of industrial biogas-CO<sub>2</sub> in a trickle-bed reactor. *J. CO<sub>2</sub> Util.* 51,  
431 101611. <https://doi.org/10.1016/j.jcou.2021.101611>

432 Jønson, B.D., Tsapekos, P., Tahir Ashraf, M., Jeppesen, M., Ejbye Schmidt, J., Bastidas-Oyanedel, J.-R.,  
433 2022. Pilot-scale study of biomethanation in biological trickle bed reactors converting impure  
434 CO<sub>2</sub> from a Full-scale biogas plant. *Bioresour. Technol.* 365, 128160.  
435 <https://doi.org/10.1016/j.biortech.2022.128160>

436 Kiener, A., Leisinger, T., 1983. Oxygen Sensitivity of Methanogenic Bacteria. *Syst. Appl. Microbiol.* 4,  
437 305–312. [https://doi.org/10.1016/S0723-2020\(83\)80017-4](https://doi.org/10.1016/S0723-2020(83)80017-4)

438 Laguillaumie, L., Peyre-Lavigne, M., Grimalt-Aleman, A., Gavala, H.N., Skiadas, I.V., Paul, E., Dumas,  
439 C., 2023. Controlling the microbial competition between hydrogenotrophic methanogens and

440 homoacetogens using mass transfer and thermodynamic constraints. *J. Clean. Prod.* 414,  
441 137549. <https://doi.org/10.1016/j.jclepro.2023.137549>

442 Lecker, B., Illi, L., Lemmer, A., Oechsner, H., 2017. Biological hydrogen methanation – A review.  
443 *Bioresour. Technol.* 245, 1220–1228. <https://doi.org/10.1016/j.biortech.2017.08.176>.

444 Lu, Z., Imlay, J.A., 2021. When anaerobes encounter oxygen: mechanisms of oxygen toxicity, tolerance  
445 and defence. *Nat. Rev. Microbiol.* 19, 774–785. <https://doi.org/10.1038/s41579-021-00583-y>

446 Magdalena, J.A., Angenent, L.T., Usack, J.G., 2022. The Measurement, Application, and Effect of  
447 Oxygen in Microbial Fermentations: Focusing on Methane and Carboxylate Production. *Fermentation*  
448 8, 138. <https://doi.org/10.3390/fermentation8040138>

449 Martin, A., Trinke, P., Pham, C.V., Bühler, M., Bierling, M., Holzapfel, P.K.R., Bensmann, B., Thiele, S.,  
450 Hanke-Rauschenbach, R., 2021. On the Correlation between the Oxygen in Hydrogen Content  
451 and the Catalytic Activity of Cathode Catalysts in PEM Water Electrolysis. *J. Electrochem. Soc.*  
452 168, 114513. <https://doi.org/10.1149/1945-7111/ac38f6>

453 Orgill, J.J., Atiyeh, H.K., Devarapalli, M., Phillips, J.R., Lewis, R.S., Huhnke, R.L., 2013. A comparison of  
454 mass transfer coefficients between trickle-bed, hollow fiber membrane and stirred tank  
455 reactors. *Bioresour. Technol.* 133, 340–346. <https://doi.org/10.1016/j.biortech.2013.01.124>

456 Pedizzi, C., Regueiro, L., Rodriguez-Verde, I., Lema, J.M., Carballa, M., 2016. Effect of oxygen on the  
457 microbial activities of thermophilic anaerobic biomass. *Bioresour. Technol.* 211, 765–768.  
458 <https://doi.org/10.1016/j.biortech.2016.03.085>

459 Rafrafi, Y., Laguillaumie, L., Figueras, J., Dumas, C., 2021. Correction to: Biological Methanation of H<sub>2</sub>  
460 and CO<sub>2</sub> with Mixed Cultures: Current Advances, Hurdles and Challenges. *Waste Biomass*  
461 *Valorization* 12, 5283. <https://doi.org/10.1007/s12649-021-01346-9>

462 Rodin, V., Lindorfer, J., Böhm, H., Vieira, L., 2020. Assessing the potential of carbon dioxide  
463 valorisation in Europe with focus on biogenic CO<sub>2</sub>. *J. CO<sub>2</sub> Util.* 41, 101219.  
464 <https://doi.org/10.1016/j.jcou.2020.101219>

465 Schill, N., van Gulik, W.M., Voisard, D., von Stockar, U., 1996. Continuous cultures limited by a gaseous  
466 substrate: Development of a simple, unstructured mathematical model and experimental  
467 verification with *Methanobacterium thermoautotrophicum*. *Biotechnol. Bioeng.* 51, 645–658.  
468 [https://doi.org/10.1002/\(SICI\)1097-0290\(19960920\)51:6<645::AID-BIT4>3.0.CO;2-H](https://doi.org/10.1002/(SICI)1097-0290(19960920)51:6<645::AID-BIT4>3.0.CO;2-H)

469 Seedorf, H., Dreisbach, A., Hedderich, R., Shima, S., Thauer, R.K., 2004. F420H<sub>2</sub> oxidase (FprA) from  
470 *Methanobrevibacter arboriphilus*, a coenzyme F420-dependent enzyme involved in O<sub>2</sub>  
471 detoxification. *Arch. Microbiol.* 182, 126–137. <https://doi.org/10.1007/s00203-004-0675-3>

472 Strübing, D., Huber, B., Lebuhn, M., Drewes, J.E., Koch, K., 2017. High performance biological  
473 methanation in a thermophilic anaerobic trickle bed reactor. *Bioresour. Technol.* 245, 1176–  
474 1183. <https://doi.org/10.1016/j.biortech.2017.08.088>

475 Thema, M., Bauer, F., Sterner, M., 2019. Power-to-Gas: Electrolysis and methanation status review.  
476 *Renew. Sustain. Energy Rev.* 112, 775–787. <https://doi.org/10.1016/j.rser.2019.06.030>

477 Tholen, A., Pester, M., Brune, A., 2007. Simultaneous methanogenesis and oxygen reduction by  
478 *Methanobrevibacter cuticularis* at low oxygen fluxes. *FEMS Microbiol. Ecol.* 62, 303–312.  
479 <https://doi.org/10.1111/j.1574-6941.2007.00390.x>

480 Trinke, P., Bensmann, B., Hanke-Rauschenbach, R., 2017. Experimental evidence of increasing oxygen  
481 crossover with increasing current density during PEM water electrolysis. *Electrochem.*  
482 *Commun.* 82, 98–102. <https://doi.org/10.1016/j.elecom.2017.07.018>

483 Vinardell, S., Feickert Fenske, C., Heimann, A., Cortina, J.L., Valderrama, C., Koch, K., 2024. Exploring  
484 the potential of biological methanation for future defossilization scenarios: Techno-economic  
485 and environmental evaluation. *Energy Convers. Manag.* 307, 118339.  
486 <https://doi.org/10.1016/j.enconman.2024.118339>

487 Yu, N., Guo, B., Zhang, Y., Zhang, L., Zhou, Y., Liu, Y., 2020. Different micro-aeration rates facilitate  
488 production of different end-products from source-diverted blackwater. *Water Res.* 177,  
489 115783. <https://doi.org/10.1016/j.watres.2020.115783>

490

491 **Supplementary data**

492 Table S1: Gas input composition for a biomethanation plant from CO<sub>2</sub>-rich off-gas (column 2) or raw  
 493 biogas (column 3). The data are from a digester producing 91 Nm<sup>3</sup>/h biomethane (Ariège  
 494 Biomethane, Arkolia Energies, France).

| Compound               | Off-gas | Raw biogas |
|------------------------|---------|------------|
| CO <sub>2</sub> (%)    | 98.90   | 44.5       |
| CH <sub>4</sub> (%)    | 0.80    | 55.0       |
| O <sub>2</sub> (%)     | 0.20    | 0.1        |
| N <sub>2</sub> (%)     | 0.01    | 0.4        |
| H <sub>2</sub> O (%)   | 0.18    | 0.8        |
| H <sub>2</sub> S (ppm) | <10     | 100        |

495  
 496  
 497  
 498

Table S2: Inoculum elemental content in the soluble phase measured by ICP-MOES.

| Element | Concentration (mg/L) |
|---------|----------------------|
| S       | 54.3                 |
| Na      | 60                   |
| K       | 78                   |
| P       | 32                   |
| Ca      | 46                   |
| Mg      | 3.88                 |
| Fe      | 0.820                |
| Ni      | 0.670                |
| Co      | 0.120                |
| Zn      | 1.19                 |
| Cu      | 1.370                |
| Se      | 0.189                |

499  
 500

501

Table S3: Composition of nutrient solutions S1 and S2 for continuous reactor

| <b>Solution</b> | <b>Compound</b>                                     | <b>Concentration<br/>(mg/L)</b> |
|-----------------|---|---------------------------------|
| S1              | NH <sub>4</sub> OH                                  | 8045.5                          |
|                 | K <sub>2</sub> HPO <sub>4</sub>                     | 319.1                           |
|                 | CaCl <sub>2</sub> ·2H <sub>2</sub> O                | 320.0                           |
|                 | MgCl <sub>2</sub> ·6H <sub>2</sub> O                | 63.6                            |
|                 | FeCl <sub>3</sub>                                   | 8.3                             |
|                 | NiCl <sub>2</sub> ·6H <sub>2</sub> O                | 6.7                             |
|                 | CoCl <sub>2</sub> ·6H <sub>2</sub> O                | 1.60                            |
|                 | Na <sub>2</sub> O <sub>3</sub> Se·5H <sub>2</sub> O | 3.3                             |
|                 | Na <sub>2</sub> O <sub>4</sub> W·2H <sub>2</sub> O  | 5.80                            |
| S2              | Na <sub>2</sub> S·9H <sub>2</sub> O                 | 360                             |

502

503

504

505